LANGMUIR

pubs.acs.org/Langmuir Article

Probing the Mechanism of Antibody-Triggered Aggregation of Gold Nanoparticles

Samuel Okyem, Olatunde Awotunde, Tosin Ogunlusi, McKenzie B. Riley, and Jeremy D. Driskell*

Cite This: https://dx.doi.org/10.1021/acs.langmuir.1c00100 Read Online

ACCESS | Metrics & More | Article Recommendations | Supporting Information

ABSTRACT: The unique physicochemical properties of gold nanoparticles (AuNPs) provide many opportunities to develop novel biomedical technologies. The surface chemistry of AuNPs can be engineered to perform a variety of functions, including targeted binding, cellular uptake, or stealthlike properties through the immobilization of biomolecules, such as proteins. It is well established that proteins can spontaneously adsorb onto AuNPs, to form a stable and functional bioconjugate; however, the protein−AuNP interaction may result in the formation of less desirable protein−AuNP aggregates. Therefore, it is imperative to investigate the protein−AuNP interaction and elucidate the mechanism by which protein triggers AuNP aggregation. Herein, we systematically investigated the interaction of immunoglobulin G (IgG) antibody with citrate-capped AuNPs as a function of solution pH. We found that the addition of antibody triggers the aggregation of AuNPs for pH < 7.5, whereas a monolayer of antibody adsorbs onto the AuNP to form a stable bioconjugate when the antibody is added to AuNPs at pH ≥ 7.5. Our data identifies electrostatic bridging between the antibody and the negatively charged AuNPs as the mechanism by which aggregation occurs and rules out protein unfolding and surface charge depletion as potential causes. Furthermore, we found that the electrostatic bridging of AuNPs is reversible within the first few hours of interaction, but the protein−AuNP interactions strengthen over 24 h, after which the protein−AuNP aggregate is irreversibly formed. From this data, we developed a straightforward approach to acrylate the basic residues on the antibody to prevent protein-induced aggregation of AuNP over a wide pH range. The results of this study provide additional insight into antibody−nanoparticle interactions and provide a pathway to control the interaction with the potential to enhance the conjugate function.

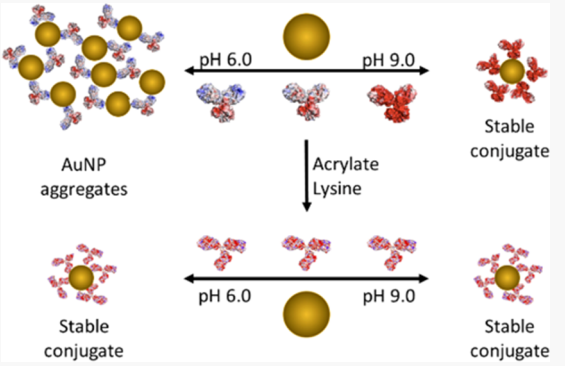

Downloaded via ILLINOIS STATE UNIV on March 8, 2021 at 17:40:09 (UTC).
See https://pubs.acs.org/sharingguidelines for options on how to legitimately share published articles.

INTRODUCTION

Gold nanoparticles (AuNPs) have remarkable physicochemical properties and high biocompatibility, and with properly engineered surface functionalization, they have been exploited in many emerging biomedical applications,[1−6] including drug delivery,[7] photothermal therapy,[8] tissue imaging,[9] and disease diagnosis.[10] The surface chemistry of AuNPs allows it to adsorb several biomolecules, such as proteins, to form functional bioconjugates. Although many proteins form stable conjugates with AuNPs, protein adsorption can trigger nanoparticle aggregation. For example, bovine serum albumin (BSA) and immunoglobulin G (IgG) have been shown to form stable conjugates with AuNPs at physiological pH,[11,12] while lysozyme and other proteins induce AuNP aggregation at physiological pH.[13,14] To this point, it becomes relevant to understand the fundamental mechanism by which these aggregations occur, to synthesize stable protein−AuNP conjugates for use in a biomedical application and avoid in vivo detrimental effects caused by aggregates.[15]

Our group, as well as others, are specifically interested in the adsorption of IgG antibody onto AuNPs to form highly stable and functional conjugates for nanoparticle-enabled sensing applications.[16−22] In previous work, IgG molecules were found to irreversibly adsorb onto citrate-capped AuNPs and resist displacement from the AuNP surface by serum proteins.[23] This irreversible adsorption was attributed to the substantial number of cysteine residues presented by the IgG molecule.[24−28] Additional studies have established that protein charge governs orientation upon adsorption to AuNPs, thereby influencing the function of the bioconjugate.[20,29−31] For example, as the solution pH decreases, IgG orientation on the AuNP becomes more favorable to increase the antigen-binding activity of the conjugates; however, below pH 7.5, the protein induces the aggregation of AuNPs during conjugation.[30] Thus, a detailed understanding of this antibody-induced AuNP aggregation mechanism is needed to ensure aggregation is avoided and potentially identify a pathway to synthesize stable, oriented, and highly functional conjugates facilitated by low pH.

Received: January 12, 2021
Revised: February 9, 2021

© XXXX American Chemical Society

Several mechanisms have been proposed for protein-induced nanoparticle aggregation.[13,14,32−37] For some proteins, aggregation of AuNPs is ascribed to the unfolding of protein upon adsorption followed by destabilization of the conjugate.[14,34] Zhang et al. first reported that lyzosyme undergoes a conformational change upon adsorption to AuNPs at physiological pH and that the partially unfolded protein promotes the formation of large amorphous protein−AuNP aggregates.[14] Similarly, it was reported that, at low concentrations, BSA unfolds upon adsorption to gold nanorods and induces aggregation.[34] Alternatively, other scientific evidence suggests that proteins may trigger nanoparticle aggregation by an electrostatic bridging mechanism.[32,33] For this mechanism, exposed positive charges on proteins act as an electrostatic bridge to crosslink negatively charged nanoparticles, e.g., citrate-capped AuNPs. While much of the evidence for electrostatic bridging was generated with silica nanoparticles, a few reports have attributed protein-induced aggregation of AuNPs to this mechanism.[13,36] Finally, it is possible that the protein remains folded, does not electrostatically crosslink particles, and adsorbs to form a protein monolayer; however, van der Waals attraction of nanoparticles resulting from surface modification triggers conjugate aggregation. The extended Derjaguin−Landau−Verwey−Overbeek (xDLVO) theory predicts that surface charge depletion upon protein adsorption reduces the electrostatic repulsive forces responsible for conjugate stability, and the osmotic potential increases to aid in conjugate stability.[38−40] The relative contribution of each parameter and the overall stability of the conjugate is difficult to accurately predict,[40] but allows for the possibility of protein-triggered AuNP aggregation if the electrostatic repulsion is impacted to a greater extent than the osmotic potential such that the van der Waals forces (attractive forces) overcome the repulsive forces. Collectively, these previous works establish that different proteins can trigger nanoparticle aggregation by different mechanisms; thus, it is imperative to identify commonalities among proteins that follow the same mechanism. Only then can a predictive model be developed for protein−nanoparticle interactions to direct conjugate design strategies.

In this work, we specifically investigate the interaction of IgG antibody with citrate-capped AuNPs as a function of pH. Several analytical techniques have been employed, including extinction spectrophotometry, dynamic light scattering (DLS), and ζ-potential measurements, to elucidate which, if any, of the previously described mechanisms drives the aggregation of antibody−AuNP conjugates. Following mechanistic studies, we identified a facile strategy to chemically modify the antibody using established chemistry to eliminate the pH-dependent aggregation. Our findings also suggest that the initial interaction between the antibody and AuNP is weak and reversible; however, with the increased contact time, the protein−AuNP interaction hardens and is irreversible.[26,28,41,42] Outcome of this work will drive design strategies and aid in troubleshooting the synthesis of antibody−AuNP conjugates that are widely adopted in emerging nanobiotechnology applications.

MATERIALS AND METHODS

Reagents. Citrate-capped AuNPs with a nominal diameter of 60 nm and concentration of 2.6×10^{10} particles/mL were used in all analyses. All antibody studies were performed using a mouse monoclonal anti-horseradish peroxidase IgG (anti-HRP; clone 2H11) obtained from MyBioSource. Horseradish peroxidase (HRP) and 2,2′-azino-bis-(3-ethylbenzothiazoline-6-sulfonic acid) (1-Step ABTS) were obtained from Thermo Scientific (Rockford, IL). Phosphate buffers were prepared using anhydrous potassium phosphate dibasic and potassium phosphate monohydrate purchased from Mallinckrodt Chemicals, Inc. (Paris, KY) and Fischer Scientific (Fair Lawn, NJ), respectively. All solutions were prepared using nanopure deionized water from a Barnstead water purification system (Thermo Scientific, Rockford, IL).

Antibody Preparation at Different pHs. A solution of anti-HRP antibody was prepared at 2 mg/mL in 2 mM phosphate buffer (pH 7.5). A 50 μL aliquot of the antibody was diluted to 500 μL with buffers at pH 5, 6, 7, 7.5, 8, and 9. The resulting anti-HRP antibody solutions were concentrated using an Amicon filter (MWC 100 kDa) by centrifugation at 14 000*g* for 10 min to an approximate volume of 20 μL. The concentrates were collected following results of the manufacturer's recommendation. The concentration of antibodies resuspended in buffers of different pH was determined by a NanoDrop 2000 (Thermo Scientific). A 90% recovery was achieved consistently. Recovered antibodies were further diluted to 1 mg/mL in 2 mM buffer at the appropriate pH and the hydrodynamic diameter was measured to confirm that the antibody did not aggregate as a result of solution pH.

Antibody−AuNP Synthesis at Different pHs. AuNP−antibody conjugates were synthesized by first centrifuging 100 μL of AuNPs at 5000*g* for 5 min. Nanoparticle pellets were resuspended in 100 μL of 2 mM phosphate buffer of pH 6.0, 6.5, 7.0, 7.5, 8.0, and 8.5. It was necessary to keep the buffer concentration and ionic strength low to prevent aggregation of the unconjugated AuNPs prior to adsorption of the protective antibody layer. Antibody (3 μg) was added to 100 μL of AuNPs at each pH in a low-binding microcentrifuge tube for 3 h with gentle agitation. This ratio of antibody to AuNP was selected to ensure the formation of a full monolayer of antibody on the AuNP.[30] After incubation, the AuNP−antibody suspension was centrifuged at 5000*g* for 5 min to pellet the formed conjugates. The supernatant was discarded to remove excess antibodies not adsorbed onto the AuNPs followed by resuspension of the conjugates in buffer of the same pH. The conjugates were further purified by performing the centrifuging/resuspension cycle three times.

Antibody−AuNP Conjugate Buffer Exchange. Stable purified AuNP−antibody conjugate synthesized at pH 8.0 was centrifuged at 5000*g* for 5 min. The supernatant was discarded, whereas the pelleted conjugates were resuspended in a 2 mM buffer at pH 6.0 or 6.5 and allowed to stand for 4 or 24 h. The pH of AuNP−antibody suspension after buffer exchange was initially assessed with pH paper and confirmed with a pH microelectrode.

Antigen-Binding Activity of Antibody−AuNP Conjugates. Antigen-binding capacity of the conjugates was measured to determine the impact of AuNPs on antibody unfolding. To this end, we employed an established immunoassay technique to assess the antigen capture activity of antibodies adsorbed onto AuNPs.[43] Purified AuNP−antibody conjugates (100 μL) were incubated with 3 μg of HRP for 1 h. After incubation, excess uncaptured HRP was removed by centrifuging at 5000*g* for 5 min. The conjugates saturated with bound HRP were further washed three times to ensure the removal of all free HRP. ABTS (150 μL) was mixed with the conjugates (10 μL) and the enzymatic activity of HRP captured by the conjugates was quantified by the spectrophotometric analysis of the colored product ($ABTS^+$). The concentration of HRP captured by the conjugates was determined from a calibration curve generated from the analysis of the standard solutions of HRP.

Chemical Modification of Antibody. Anti-HRP antibody was modified with *N*-succinimidyl acrylate (NSA) to acrylate the lysine residues. NSA (2 μL at 50 mM) was added to 50 μg of anti-HRP antibody and allowed to react for 2 h at room temperature with gentle shaking. Excess unreacted NSA was removed using an Amicon Ultra Centrifuging filters (MWCO 100 kDa). Five hundred microliters of 2 mM phosphate buffer pH 7.5 was used to rinse out glycerol on the filter membrane by centrifuging at 10 000*g* for 5 min. The antibody/NSA reaction mixture was diluted to 500 μL and centrifuged at 14 000*g* for 12 min. The filter was inverted and centrifuged at 1000*g* for 3 min to recover modified antibodies. A NanoDrop 2000C spectrophotometer (Thermo Scientific, Rockford, IL) was used to measure the concentration of modified antibodies. The chemical modification was

https://dx.doi.org/10.1021/acs.langmuir.1c00100
Langmuir XXXX, XXX, XXX−XXX

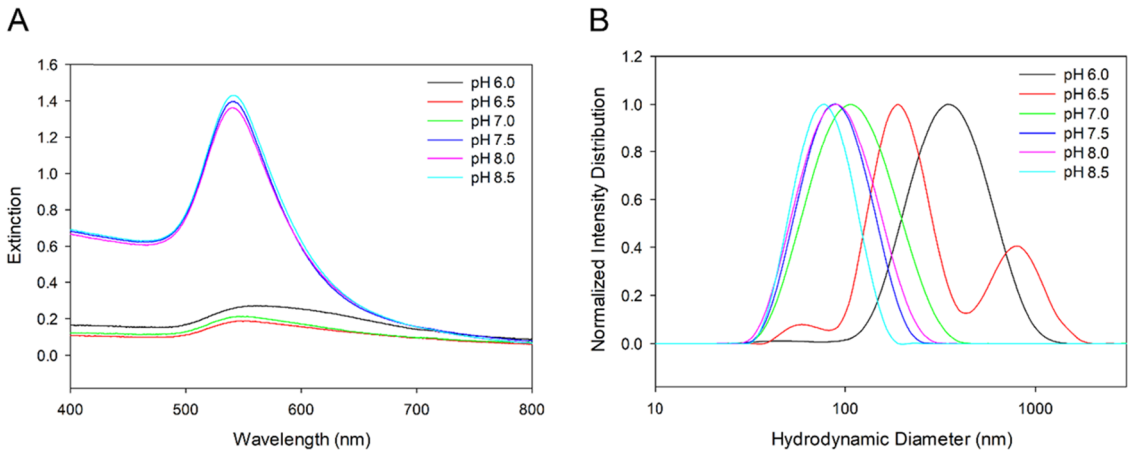

Figure 1. Evaluating the stability of antibody−AuNP conjugates at pH 6.0−8.5. (A) UV−visible extinction spectra of antibody−AuNP conjugates synthesized at different pH by adding excess antibodies to AuNP and incubating for 4 h. (B) DLS measured size distribution of antibody−AuNP conjugates synthesized at pH 6−8.5.

confirmed by measuring the ζ-potential of the antibody before and after chemical modification.

Antibody−AuNP Characterization and Stability Analysis. *Ultraviolet−Visible (UV−Vis) Characterization.* Extinction spectra of the AuNP−antibody conjugates were acquired to evaluate the stability of the conjugates using a Cary 1 Bio UV−visible dual-beam spectrophotometer with a spectral bandwidth of 0.1 nm. For this experiment, 80 μL of the conjugate was introduced into a microcuvette, after which a UV−vis scan was obtained from 350 to 900 nm at 0.5 nm increments. An iMark microplate reader (Bio-Rad) was used to assess the HRP enzymatic assay by monitoring the absorbance of the formed product at 415 nm at 10 s intervals for 20 min.

DLS Size and ζ-Potential Measurements. A Malvern Zetasizer Nano ZSP operating with noninvasive backscatter optics was used to carryout conjugate size and ζ-potential measurements. A folded capillary cuvette was filled with the appropriate buffer followed by a careful introduction of 20 μL of the conjugate to the bottom of the cuvette by the aid of a capillary pipette tip. Before size and ζ-potential measurements, the conjugates were equilibrated at 25 °C for 30 s. Conjugate size and ζ-potential measurements were performed in triplicate, and each measurement consisted of the analysis sequence of size-ζ potential-size. This sequence was adopted to confirm no aggregates were generated during the ζ-potential measurement. For each size and ζ-potential measurement, 15 separate runs were averaged.

RESULTS AND DISCUSSION

Effect of pH on Antibody-Triggered Aggregation of AuNPs. To evaluate the impact of pH on the interaction between anti-HRP antibody and AuNPs, we prepared a series of AuNP suspensions in 2 mM phosphate buffers ranging from pH 6.0 to 8.5 and added equivalent amounts of anti-HRP antibody to each pH-adjusted AuNP suspension. The mixtures were visually inspected for color and analyzed via UV−visible spectrophotometry and DLS to assess AuNP stability and the formation of antibody−AuNP conjugates. Each AuNP suspension remained red following pH adjustment (Figure S1); however, an immediate and obvious pH-dependent color change was observed following the addition of antibody. Mixtures prepared at pH $\leq$ 7.0 turned purple immediately following the addition of antibody, whereas mixtures prepared at pH $\geq$ 7.5 maintained the red color of the unconjugated AuNP suspension. This color change from red to purple is indicative of AuNP aggregation and establishes that anti-HRP antibody induces the aggregation of AuNP at a pH $\leq$ 7.0, while the protein does not trigger AuNP aggregation at pH $\geq$ 7.5.[13,44]

The extinction spectra for the antibody−AuNP mixtures at each pH were collected 4 h after the addition of the protein and are presented in Figure 1A. The extinction maximum of the antibody−AuNP mixture at pH $\geq$ 7.5 red-shifted 7 nm to 542 nm relative to the unconjugated AuNP (λ_{max} = 535 nm). This shift in extinction maximum is due to a change in the local refractive index at the AuNP surface and is the characteristic of the adsorption of antibody onto the surface of the AuNP.[45,46] Moreover, the extinction bandwidth does not broaden at pH $\geq$ 7.5, confirming the formation of monodisperse conjugates. At pH $\leq$ 7.0, the extinction band is substantially red-shifted, diminished at 542 nm, and broadened, indicating that the AuNPs aggregate. The antibody−AuNP mixtures were further analyzed via DLS to confirm pH-dependent aggregation (Figure 1B). A mean hydrodynamic diameter of 87 $\pm$ 4 nm was recorded for AuNP−antibody conjugates formed at pH 7.5 and above. This size increase reflects monolayer coverage of IgG antibody and is consistent with previous reports on the synthesis of stable, monodisperse antibody−AuNP conjugates.[11] AuNP aggregates with mean sizes greater than 200 nm were observed for protein−AuNP mixtures below pH 7.5 and corroborate the conclusions drawn from the color changes and extinction spectra.

It is well established that proteins can spontaneously adsorb onto the surface of gold nanoparticles through electrostatic interactions, Au−S chemisorption via native cysteine residues, and entropic effects.[26] Protein adsorption onto nanoparticles often forms a stable conjugate; however, as shown in Figure 1, the association of the proteins with the AuNP alters the stability of the AuNP under certain conditions, such as pH $\leq$ 7.0. Three mechanisms for protein-triggered aggregation of nanoparticles have been previously reported. First, upon adsorption to the AuNP, the protein could unfold, thereby exposing the hydrophobic regions of the protein adlayer to result in AuNP aggregation.[14,34] Second, the displacement of the citrate capping agent by less charged protein could result in surface charge depletion, which is required for nanoparticle stability as detailed by the xDLVO theory.[38−40] Third, electrostatic bridging of the negatively charged citrate-capped AuNP by the regions of positive surface charge on the protein has been described as a potential mechanism for protein-induced AuNP aggregation.[13,32,33,36]

Molecular simulations of antibody surface charge support the possibility of electrostatic bridging or surface charge depletion as

https://dx.doi.org/10.1021/acs.langmuir.1c00100
Langmuir XXXX, XXX, XXX−XXX

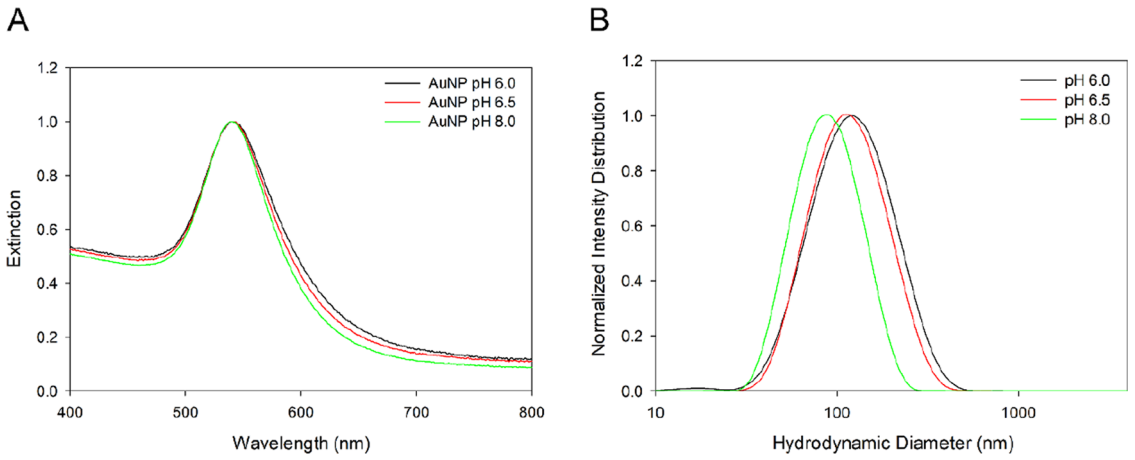

Figure 2. Extinction spectra (A) and DLS measured size distribution (B) of antibody−AuNP conjugates synthesize at pH 8.0 and resuspended at pH 6.0, 6.5, and 8.0. Conjugates were aged 4 h in a final buffer prior to analysis.

the cause for protein-triggered AuNP aggregation. As shown in Figure S2, with red and blue indicating regions of negative and positive charges, respectively, pH has a significant impact on IgG surface charge over a relatively small pH range of 6.0−7.5.[47] As expected, the positive charge increases with decreasing pH as a result of protonating the basic amino acids ubiquitous to IgG. Considering the pK_as of the amino acid side chains, it is likely that the imidazole on the histidine residues undergoes protonation/deprotonation to modulate protein charge in the pH range of 6.0−8.0, while the amine on the lysine residues is primarily protonated. Thus, the negative charge of the citrate-capped may be offset upon adsorption of the more positively charged antibody at pH $\leq$ 7.0, resulting in AuNP aggregation. Unfortunately, aggregation of the conjugates at these lower pHs prevented the accurate determination of the conjugate ζ-potential. Alternatively, the increase in positive regions on the antibody macromolecule at lower pHs (Figure S2) could result in the electrostatic bridging of two AuNPs to form aggregates. DLS analysis of purified protein solutions shows no evidence of unfolding in each pH solution prior to adsorption on the AuNP with the protein measuring 11 $\pm$ 2 nm independent of the solution pH. Admittedly, unfolding may be induced upon interaction with the AuNP surface to trigger AuNP aggregation; however, this mechanism seems unlikely given that the data in Figure 1 confirm that the antibody adsorbs onto the AuNP at pH $\geq$ 7.5 without aggregating. The following sections aim to elucidate the mechanism for antibody-triggered aggregation at lower pHs. Once the causative mechanism is identified, approaches can be taken to mitigate the effect and facilitate conjugation at lower pHs, which may lead to improved antibody orientation or greater antigen-binding activity.[20,29,30]

Buffer Exchange of Stable Antibody−AuNPs to Lower pH. To differentiate between surface charge depletion and electrostatic bridging as the source of protein-triggered AuNP aggregation, a stable conjugate was first synthesized at pH 8.0. After allowing 1 h for antibody to adsorb onto the AuNP, the conjugate was centrifuged, the supernatant was decanted, and the conjugates were resuspended in pH 6.0, 6.5, or 8.0 buffer. Buffer exchange to lower pH after the formation of a stable conjugate at pH 8.0 was conducted to alter the surface charge of the adsorbed protein, which, in effect, decreases the overall net charge of the conjugates. We anticipated that if the mechanism of protein-triggered aggregation proceeds by the reduction of the nanoparticle surface charge, which would reduce the diffusion bilayer thickness, then the nanoparticles are expected to aggregate upon titration to lower pH. Conversely, if electrostatic bridging is responsible for protein-triggered aggregation, we expect that the conjugates formed at pH 8.0 would be stable when resuspended at pH 6.0 and 6.5 since the gold surface would already be saturated and unavailable to interact with the positive regions on neighboring conjugates. Extinction spectra were collected 4 h after the conjugates were resuspended in pH 6.0 and 6.5 buffers (Figure 2A). Interestingly, the extinction bands are not red-shifted and are only slightly broadened relative to that collected for the stable conjugate formed at pH 8.0. The conjugates had mean hydrodynamic diameters of 96 $\pm$ 1, 97 $\pm$ 1, and 82 $\pm$ 2 nm when resuspended at pH 6.0, 6.5, and 8.0, respectively (Figure 2B). The conjugates remained stable for at least 24 h, although it is worth noting that some of the conjugates adsorbed to the walls of the microcentrifuge tube as the pH decreased (Figure S3). DLS is known to overestimate the mean particle sizes for a population even with trace levels of larger aggregates given its inherent bias for detecting larger aggregates that scatter light more efficiently;[48] thus, the minimal increase in mean size is likely due to the presence of a few aggregates in the overwhelmingly stable antibody−AuNP suspension. It is well established that protein monolayers are not close-packed and often require additional blocking agents to passivate unmodified regions on the surface; thus, the formation of a few aggregates can be rationalized as the crosslinking of two conjugates where the adsorbed antibody on one conjugate binds to a region of unmodified gold due to poor monolayer packing on another conjugate, i.e., electrostatic bridging. Nevertheless, the stability of these conjugates is in stark contrast to the addition of antibody to unconjugated AuNP at pHs 6.0 and 6.5, and these results indicate that the preformed, stable conjugates do not aggregate after titration to lower pHs.

Collectively, these results suggest that the reduction of the net nanoparticle surface charge by adsorbed antibodies is not the prevalent mechanism that causes nanoparticles to aggregate at pH $\leq$ 7.0. When stable conjugates synthesized at pH 8.0 are resuspended in a lower pH buffer, the net charge on the conjugates is reduced (Figure S4) as anticipated as more ionizable side chains are protonated. While the electrostatic potential decreases upon resuspension of conjugates in a buffer of lower pH, the xDLVO theory suggests that the adsorbed protein layer provides additional elastic and osmotic poten-

https://dx.doi.org/10.1021/acs.langmuir.1c00100
Langmuir XXXX, XXX, XXX−XXX

tials.[39,40] These repulsive forces from adsorbed antibody contribute to the overall surface potential, which prevent the antibody−AuNP conjugate from aggregating.

The antigen-binding activity of the conjugates was measured to confirm that the antibody did not denature at lower pHs or upon adsorption on the AuNP. As noted above, the unfolding of proteins upon adsorption onto nanoparticles has also been proposed as one of the mechanisms that can drive nanoparticle aggregation;[14,34] thus, we aimed to definitively rule out this pathway to aggregation. Hypothesizing that the antigen-binding capabilities of antibodies will be lost if the antibody unfolds, we implemented a previously developed enzyme-based assay to quantify the antigen-binding activity of the conjugate.[43] Here, stable, purified anti-HRP antibody−AuNP conjugates were resuspended in buffer at pH 6.0, 6.5, and 8.0 for 24 h and mixed with an excess of HRP to saturate all available binding sites on the conjugates. The enzymatic activity of HRP captured by conjugates was analyzed to quantify the number of active binding sites presented by the antibodies adsorbed onto the AuNP. Figure 3 shows that antibody−AuNP conjugates were

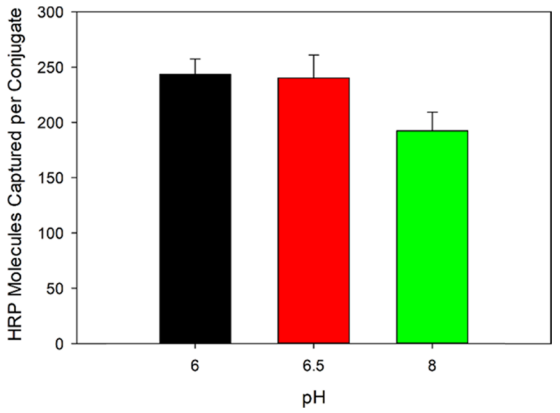

Figure 3. Quantitation of antigen-binding activity of conjugates after resuspension into a buffer of pH 6.0, 6.5, and 8.0. Antibody−AuNP conjugate synthesized at pH 8.0 is resuspended in a buffer of pH 6.0, 6.5, and 8.0 for 24 h.

highly active at each pH, capturing >200 HRP molecules per conjugate, and the slightly greater antigen-binding capacity of the conjugate at pHs 6.0 and 6.5 compared to pH 8.0 potentially arises from different antibody orientations.[29,30] This result suggests no drastic unfolding of antibodies adsorbed onto AuNPs that can trigger nanoparticle aggregation.

Based on the stability and activity of the conjugates after resuspension at low pH, charge depletion and protein unfolding can be ruled out as mechanisms to describe the behavior of antibody-triggered aggregation of AuNP. Therefore, these observations suggest that antibody induces AuNP aggregation at lower pHs as a result of electrostatic bridging.

Effects of Titration with NaOH on the Reversibility of Aggregates. DLS and UV−visible spectrophotometry were conducted to probe the reversibility of the AuNP aggregates formed by the addition of antibody at pH 6.0 and 6.5. The antibody was added to 100 μL of AuNPs at pH 6.5, and the aggregates were characterized after 30 min, 5 h, and 24 h of incubation at room temperature. DLS measured size distributions are presented in Figure 4A−C and show that large aggregates were observed at all time points. The persistence of these aggregates over a period of 24 h implies no propensity toward spontaneous reversibility. Extinction spectra confirm the formation of aggregates at each time point (Figure 4D−F). Subsequently, the pH was adjusted to pH 8.0 by the addition of 0.1 M NaOH to the aggregates formed after each incubation time. The sample that was allowed to incubate for 30 min immediately turned from purple to red upon the addition of 0.1 M NaOH. The hydrodynamic diameter shifted to reflect a population of monodisperse conjugates consisting of a single particle with a monolayer of antibody (Figure 4A), and the extinction spectrum corroborated the reversibility of the aggregate formation upon addition of base (Figure 4D). Similar reversible behavior was observed for the aggregates allowed to incubate for 5 h; however, there was a small but notable increase in the mean hydrodynamic diameter after the addition of NaOH to reverse the aggregation relative to the stable conjugates formed at pH 8.0 (Figure 4B,E). Most notably, a significant amount of aggregates was still present for the 24 h incubation even after the addition of 0.1 M NaOH (Figure 4C,F). Similar trends for incubation time-dependent reversible aggregation were found for the experiments performed at pH 6.0 (Figure S5).

These observations support an electrostatic bridging mechanism for antibody-induced AuNP aggregation at low pHs. We inferred that the positive patches on the antibodies initiate long-range electrostatic interactions that govern the initial protein interaction with the citrate-capped AuNP. However, this electrostatic interaction results in a loosely bound soft corona, and the protein−AuNP interaction can be reversed upon deprotonation of the antibody. Increased incubation time allows the loosely adsorbed antibody to undergo a reorientation and rearrangement process to establish a more thermodynamically stable interaction. This process of corona hardening leads to a robust and irreversible interaction between the antibody and AuNP, and this process has been previously reported.[26,28,41,42]

Mitigating Antibody-Triggered Aggregation of AuNPs. One pathway to prevent protein-triggered aggregation of AuNPs is to reduce the positive charge on the protein surface. Molecular simulations confirm that the total surface charge of proteins is determined by the number and identity of ionizable side chains of its amino acids. Primary amines of lysine residues are mostly protonated at and below physiological pH and are largely responsible for the total positive charge on the protein surface. We hypothesized that chemical modification of the surface accessible amines to introduce a neutral functional group would decrease the number of positively charged regions on the protein, thereby preventing electrostatic bridging of the AuNPs. To this end, we reacted the antibody with *N*-succinimidyl acrylate (NSA) to modify the most solvent-accessible lysine residues (Figure S6). The acrylated lysine loses the potential to possess a positive charge even at acidic pH and substantially reduces the localized positive charges on the chemically modified antibody as confirmed by molecular simulations (Figure S7).[47]

Equivalent amounts of chemically modified antibody were added to the suspensions of AuNP adjusted to pH 6.0 and 6.5 to evaluate the impact of protein acrylation on the interaction between anti-HRP antibody and AuNPs. Each conjugate remained red following the addition of the acrylated antibody, in contrast to the drastic color change observed for the addition of an unmodified antibody to AuNP at pH 6.0 and 6.5. Extinction spectra for the modified antibody−AuNP mixtures were collected 4 h after the addition of protein (Figure 5A). The extinction band is the characteristic of well-dispersed single particles, with the extinction maxima observed at 538 and 537

https://dx.doi.org/10.1021/acs.langmuir.1c00100
Langmuir XXXX, XXX, XXX−XXX

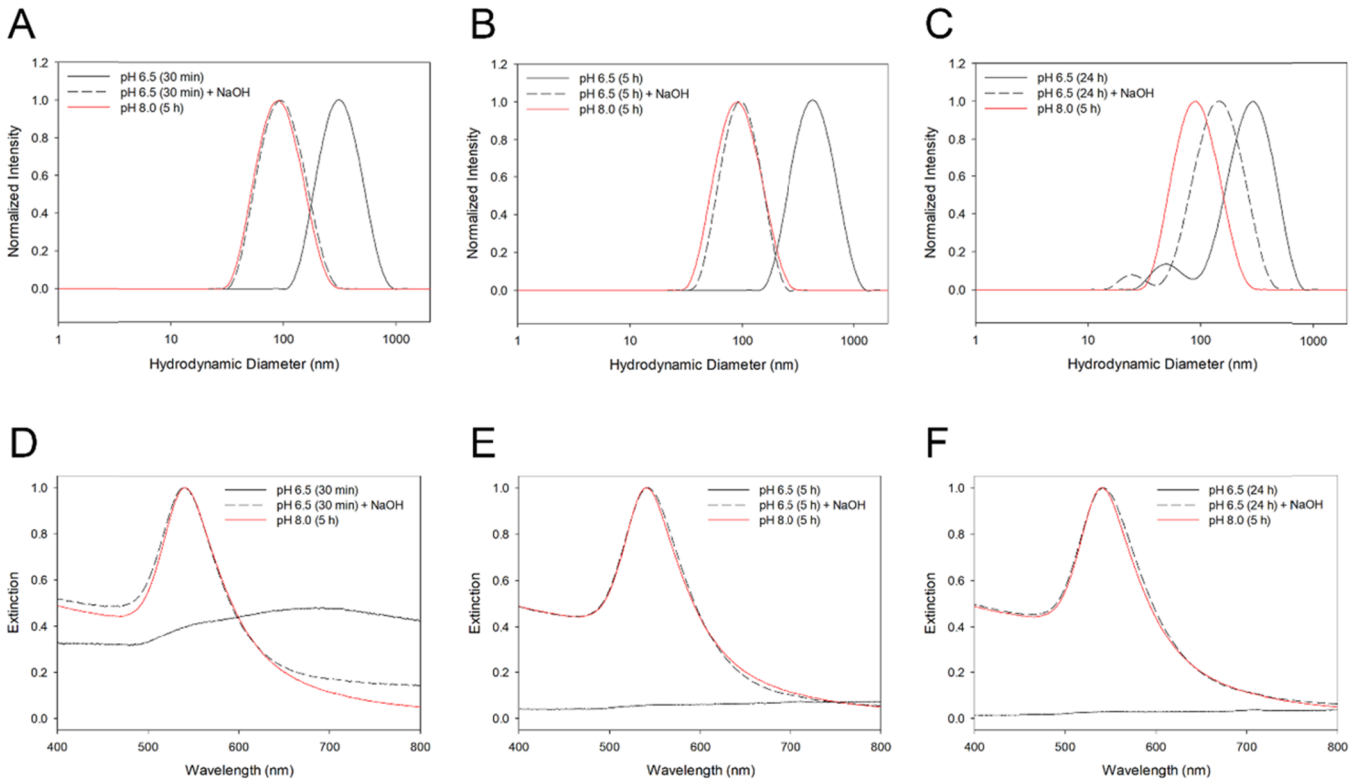

Figure 4. Reversibility of aggregation by addition of NaOH. DLS size distribution (A−C) and extinction spectra (D−F) of conjugates synthesized at pH 6.5 for 30 min (A and D), 5 h (B and E), or 24 h (C and F) and titrated to higher pH by addition of 0.1 M NaOH. Red lines represent the size distribution and extinction spectrum of antibody−AuNP conjugates formed at pH 8.0 as a reference for monodisperse conjugates.

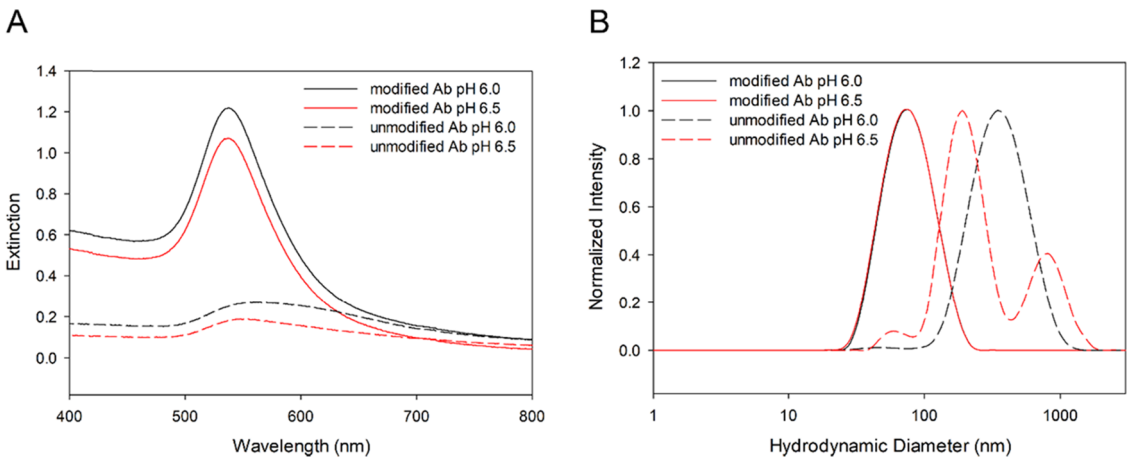

Figure 5. Synthesis of UV−visible extinction spectra (A) and DLS measured size distribution (B) of antibody−AuNP conjugates synthesized with chemically modified (acrylated) antibody at pH 6.0 and 6.5 (solid lines). Characterization of conjugates synthesized with an unmodified antibody is included as controls (dashed lines).

nm for conjugates at pH 6.0 and 6.5, respectively. DLS analysis yielded a mean hydrodynamic diameter of 69 ± 2 nm and confirmed the formation of stable conjugates with acrylated antibody at pH 6.0 and 6.5 (Figure 5B). In support of our hypothesis, these data demonstrate the ability to synthesize stable AuNP−antibody conjugates at lower pH after knocking out some of the positive charges on the antibody.

CONCLUSIONS

In summary, we studied the effect of pH on the interaction of antibody with citrate-capped AuNPs and systematically manipulated the chemical system to provide insight into the mechanism responsible for the antibody-induced aggregation of AuNPs. While several mechanisms have been proposed for protein-triggered nanoparticle aggregation, our results confirm that the protein surface charge governs antibody-triggered AuNP aggregation. Our data support electrostatic bridging as the prevalent mechanism by which antibodies induce AuNP aggregation at pH ≤ 7.5, where a single protein with multiple regions of localized positive surface charge interacts with two negatively charged AuNPs. Each AuNP can support multiple protein bridges to result in large, multiparticle aggregates. In addition to elucidating this aggregation mechanism, we demonstrated that modification of basic amino acids on the

https://dx.doi.org/10.1021/acs.langmuir.1c00100
Langmuir XXXX, XXX, XXX−XXX

protein can reduce protein surface charges to prevent AuNP aggregation and facilitate conjugate synthesis under lower pH conditions. This approach can potentially be applied to other protein systems that trigger the aggregation of AuNP or as a means to alter the orientation of proteins immobilized on the nanoparticle surface to enhance biological function.

Our studies provide additional insights into general nanoparticle stability and protein−AuNP interactions, beyond those associated with protein-induced aggregation. We reaffirm steric interactions as one of the potentials contributing to the stability of protein-functionalized AuNPs as proposed by several theoretical models.[44−46] This allows the formation of a stable conjugate under ideal solution conditions followed by the subsequent resuspension of the preformed conjugate in more diverse solution conditions that are otherwise unfavorable during the conjugate synthesis. Finally, our reversibility study shows that electrostatic forces govern the initial interaction between the protein and AuNP, but electrostatic forces are reversible. However, after aging, the protein irreversibly binds. This observation is consistent with previous reports of the formation of hard protein coronas,[26,41,42] a three-step model for protein−AuNP adsorption,[28] and the importance of thiol−AuNP interactions.[24,26]

■ ASSOCIATED CONTENT

Supporting Information

The Supporting Information is available free of charge at https://pubs.acs.org/doi/10.1021/acs.langmuir.1c00100.

Extinction spectra of AuNP in various buffers; simulation of IgG surface charge as a function of pH; extinction spectra and DLS size distribution of antibody−AuNP conjugates after 24 h buffer exchange; ζ-potential of conjugates; reversibility of aggregates formed at pH 6.0; chemical reaction for modifying lysine; and simulation of IgG surface charge after chemical modification (PDF)

■ AUTHOR INFORMATION

Corresponding Author

Jeremy D. Driskell − *Department of Chemistry, Illinois State University, Normal, Illinois 61790, United States;* orcid.org/0000-0001-5082-898X; Email: jdriske@ilstu.edu

Authors

Samuel Okyem − *Department of Chemistry, Illinois State University, Normal, Illinois 61790, United States*

Olatunde Awotunde − *Department of Chemistry, Illinois State University, Normal, Illinois 61790, United States*

Tosin Ogunlusi − *Department of Chemistry, Illinois State University, Normal, Illinois 61790, United States*

McKenzie B. Riley − *Department of Chemistry, Illinois State University, Normal, Illinois 61790, United States*

Complete contact information is available at: https://pubs.acs.org/10.1021/acs.langmuir.1c00100

Notes

The authors declare no competing financial interest.

■ ACKNOWLEDGMENTS

This work was funded by the National Science Foundation through the Macromolecular, Supramolecular, and Nanochemistry Program, Award No. CHE-1807126. O.A. and S.O. would like to thank the Illinois State University Department of Chemistry for partial support. Molecular graphics and analyses were performed with UCSF Chimera, developed by the Resource for Biocomputing, Visualization, and Informatics at the University of California, San Francisco, with support from NIH P41-GM103311.

■ REFERENCES

(1) Das, M.; Shim, K. H.; An, S. S. A.; Yi, D. K. Review on Gold Nanoparticles and Their Applications. *Toxicol. Environ. Health Sci.* **2011**, *3*, 193−205.

(2) Dreaden, E. C.; Alkilany, A. M.; Huang, X.; Murphy, C. J.; El-Sayed, M. A. The Golden Age: Gold Nanoparticles for Biomedicine. *Chem. Soc. Rev.* **2012**, *41*, 2740−2779.

(3) Dykman, L.; Khlebtsov, N. Gold Nanoparticles in Biomedical Applications: Recent Advances and Perspectives. *Chem. Soc. Rev.* **2012**, *41*, 2256−2282.

(4) Giljohann, D. A.; Seferos, D. S.; Daniel, W. L.; Massich, M. D.; Patel, P. C.; Mirkin, C. A. Gold Nanoparticles for Biology and Medicine. *Angew. Chem., Int. Ed.* **2010**, *49*, 3280−3294.

(5) Yeh, Y.-C.; Creran, B.; Rotello, V. M. Gold Nanoparticles: Preparation, Properties, and Applications in Bionanotechnology. *Nanoscale* **2012**, *4*, 1871−1880.

(6) Li, D.; Wang, F.; Di, H.; Liu, X.; Zhang, P.; Zhou, W.; Liu, D. Cross-Linked Poly(Ethylene Glycol) Shells for Nanoparticles: Enhanced Stealth Effect and Colloidal Stability. *Langmuir* **2019**, *35*, 8799−8805.

(7) Ghosh, P.; Han, G.; De, M.; Kim, C. K.; Rotello, V. M. Gold Nanoparticles in Delivery Applications. *Adv. Drug Delivery Rev.* **2008**, *60*, 1307−1315.

(8) Ali, M. R. K.; Wu, Y.; El-Sayed, M. A. Gold-Nanoparticle-Assisted Plasmonic Photothermal Therapy Advances toward Clinical Application. *J. Phys. Chem. C* **2019**, *123*, 15375−15393.

(9) Xiao, T.; Qin, J.; Peng, C.; Guo, R.; Lu, X.; Shi, X. A Dendrimer-Based Dual Radiodense Element-Containing Nanoplatform for Targeted Enhanced Tumor Computed Tomography Imaging. *Langmuir* **2020**, *36*, 3096−3103.

(10) Zhou, W.; Gao, X.; Liu, D.; Chen, X. Gold Nanoparticles for in Vitro Diagnostics. *Chem. Rev.* **2015**, *115*, 10575−10636.

(11) James, A. E.; Driskell, J. D. Monitoring Gold Nanoparticle Conjugation and Analysis of Biomolecular Binding with Nanoparticle Tracking Analysis (Nta) and Dynamic Light Scattering (Dls). *Analyst* **2013**, *138*, 1212−1218.

(12) Matei, I.; Buta, C. M.; Turcu, I. M.; Culita, D.; Munteanu, C.; Ionita, G. Formation and Stabilization of Gold Nanoparticles in Bovine Serum Albumin Solution. *Molecules* **2019**, *24*, No. 3395.

(13) Neupane, S.; Pan, Y.; Takalkar, S.; Bentz, K.; Farmakes, J.; Xu, Y.; Chen, B.; Liu, G.; Qian, S. Y.; Yang, Z. Probing the Aggregation Mechanism of Gold Nanoparticles Triggered by a Globular Protein. *J. Phys. Chem. C* **2017**, *121*, 1377−1386.

(14) Zhang, D.; Neumann, O.; Wang, H.; Yuwono, V. M.; Barhoumi, A.; Perham, M.; Hartgerink, J. D.; Wittung-Stafshede, P.; Halas, N. J. Gold Nanoparticles Can Induce the Formation of Protein-Based Aggregates at Physiological Ph. *Nano Lett.* **2009**, *9*, 666−671.

(15) Marichal, L.; Degrouard, J.; Gatin, A.; Raffray, N.; Aude, J.-C.; Boulard, Y.; et al. From Protein Corona to Colloidal Self-Assembly: The Importance of Protein Size in Protein−Nanoparticle Interactions. *Langmuir* **2020**, *36*, 8218−8230.

(16) Frimpong, R.; Jang, W.; Kim, J.-H.; Driskell, J. D. Rapid Vertical Flow Immunoassay on Aunp Plasmonic Paper for Sers-Based Point of Need Diagnostics. *Talanta* **2021**, *223*, No. 121739.

(17) Granger, J. H.; Schlotter, N. E.; Crawford, A. C.; Porter, M. D. Prospects for Point-of-Care Pathogen Diagnostics Using Surface-Enhanced Raman Scattering (SERS). *Chem. Soc. Rev.* **2016**, *45*, 3865−3882.

(18) Jans, H.; Huo, Q. Gold Nanoparticle-Enabled Biological and Chemical Detection and Analysis. *Chem. Soc. Rev.* **2012**, *41*, 2849−2866.

(19) Lopez, A.; Lovato, F.; Hwan Oh, S.; Lai, Y. H.; Filbrun, S.; Driskell, E. A.; Driskell, J. D. Sers Immunoassay Based on the Capture and Concentration of Antigen-Assembled Gold Nanoparticles. *Talanta* **2016**, *146*, 388−393.
(20) Parolo, C.; de la Escosura-Muñiz, A.; Polo, E.; Grazú, V.; de la Fuente, J. M.; Merkoçi, A. Design, Preparation, and Evaluation of a Fixed-Orientation Antibody/Gold-Nanoparticle Conjugate as an Immunosensing Label. *ACS Appl. Mater. Interfaces* **2013**, *5*, 10753−10759.
(21) Penn, M. A.; Drake, D. M.; Driskell, J. D. Accelerated Surface-Enhanced Raman Spectroscopy (Sers)-Based Immunoassay on a Gold-Plated Membrane. *Anal. Chem.* **2013**, *85*, 8609−8617.
(22) Saha, K.; Agasti, S. S.; Kim, C.; Li, X.; Rotello, V. M. Gold Nanoparticles in Chemical and Biological Sensing. *Chem. Rev.* **2012**, *112*, 2739−2779.
(23) Ruiz, G.; Ryan, N.; Rutschke, K.; Awotunde, O.; Driskell, J. D. Antibodies Irreversibly Adsorb to Gold Nanoparticles and Resist Displacement by Common Blood Proteins. *Langmuir* **2019**, *35*, 10601−10609.
(24) Awotunde, O.; Okyem, S.; Chikoti, R.; Driskell, J. D. Role of Free Thiol on Protein Adsorption to Gold Nanoparticles. *Langmuir* **2020**, *36*, 9241−9249.
(25) Siriwardana, K.; LaCour, A.; Zhang, D. Critical Sequence Dependence in Multicomponent Ligand Binding to Gold Nanoparticles. *J. Phys. Chem. C* **2016**, *120*, 6900−6905.
(26) Siriwardana, K.; Wang, A.; Vangala, K.; Fitzkee, N.; Zhang, D. Probing the Effects of Cysteine Residues on Protein Adsorption onto Gold Nanoparticles Using Wild-Type and Mutated Gb3 Proteins. *Langmuir* **2013**, *29*, 10990−10996.
(27) Vangala, K.; Ameer, F.; Salomon, G.; Le, V.; Lewis, E.; Yu, L. Y.; Liu, D.; Zhang, D. M. Studying Protein and Gold Nanoparticle Interaction Using Organothiols as Molecular Probes. *J. Phys. Chem. C* **2012**, *116*, 3645−3652.
(28) Wang, A.; Vangala, K.; Vo, T.; Zhang, D.; Fitzkee, N. C. A Three-Step Model for Protein−Gold Nanoparticle Adsorption. *J. Phys. Chem. C* **2014**, *118*, 8134−8142.
(29) Puertas, S.; Batalla, P.; Moros, M.; Polo, E.; del Pino, P.; Guisán, J. M.; Grazú, V.; de la Fuente, J. M. Taking Advantage of Unspecific Interactions to Produce Highly Active Magnetic Nanoparticle−Antibody Conjugates. *ACS Nano* **2011**, *5*, 4521−4528.
(30) Ruiz, G.; Tripathi, K.; Okyem, S.; Driskell, J. D. Ph Impacts the Orientation of Antibody Adsorbed onto Gold Nanoparticles. *Bioconjugate Chem.* **2019**, *30*, 1182−1191.
(31) Treuel, L.; Brandholt, S.; Maffre, P.; Wiegele, S.; Shang, L.; Nienhaus, G. U. Impact of Protein Modification on the Protein Corona on Nanoparticles and Nanoparticle−Cell Interactions. *ACS Nano* **2014**, *8*, 503−513.
(32) Bharti, B.; Meissner, J.; Findenegg, G. H. Aggregation of Silica Nanoparticles Directed by Adsorption of Lysozyme. *Langmuir* **2011**, *27*, 9823−9833.
(33) Bharti, B.; Meissner, J.; Klapp, S. H. L.; Findenegg, G. H. Bridging Interactions of Proteins with Silica Nanoparticles: The Influence of Ph, Ionic Strength and Protein Concentration. *Soft Matter* **2014**, *10*, 718−728.
(34) Dominguez-Medina, S.; Kisley, L.; Tauzin, L. J.; Hoggard, A.; Shuang, B.; et al. Adsorption and Unfolding of a Single Protein Triggers Nanoparticle Aggregation. *ACS Nano* **2016**, *10*, 2103−2112.
(35) Fei, L.; Perrett, S. Effect of Nanoparticles on Protein Folding and Fibrillogenesis. *Int. J. Mol. Sci.* **2009**, *10*, 646−655.
(36) Filbrun, S. L.; Mandl, A.; Lovato, F.; Oh, S. H.; Driskell, E. A.; Driskell, J. D. Chemical Modification of Antibody Enables the Formation of Stable Antibody-Gold Nanoparticle Conjugates for Biosensing. *Analyst* **2017**, *142*, 4456−4467.
(37) Neupane, S.; Pan, Y.; Li, H.; Patnode, K.; Farmakes, J.; Liu, G.; Yang, Z. Engineering Protein−Gold Nanoparticle/Nanorod Complexation Via Surface Modification for Protein Immobilization and Potential Therapeutic Applications. *ACS Appl. Nano Mater.* **2018**, *1*, 4053−4063.
(38) Verwey, E. J. W.; Overbeek, J. T. G. *Theory of the Stability of Lyophobic Colloids: The Interaction of Sol Particles Having an Electric Double Layer*; Elsevier, Amsterdam, 1948; p 205.
(39) Wijenayaka, L. A.; Ivanov, M. R.; Cheatum, C. M.; Haes, A. J. Improved Parametrization for Extended Derjaguin, Landau, Verwey, and Overbeek Predictions of Functionalized Gold Nanosphere Stability. *J. Phys. Chem. C* **2015**, *119*, 10064−10075.
(40) Xi, W. J.; Phan, H. T.; Haes, A. J. How to Accurately Predict Solution-Phase Gold Nanostar Stability. *Anal. Bioanal. Chem.* **2018**, *410*, 6113−6123.
(41) Goy-López, S.; Juárez, J.; Alatorre-Meda, M.; Casals, E.; Puntes, V. F.; Taboada, P.; Mosquera, V. Physicochemical Characteristics of Protein-Np Bioconjugates: The Role of Particle Curvature and Solution Conditions on Human Serum Albumin Conformation and Fibrillogenesis Inhibition. *Langmuir* **2012**, *28*, 9113−9126.
(42) Milani, S.; Bombelli, F. B.; Pitek, A. S.; Dawson, K. A.; Radler, J. Reversible Versus Irreversible Binding of Transferrin to Polystyrene Nanoparticles: Soft and Hard Corona. *ACS Nano* **2012**, *6*, 2532−2541.
(43) Tripathi, K.; Driskell, J. D. Quantifying Bound and Active Antibodies Conjugated to Gold Nanoparticles: A Comprehensive and Robust Approach to Evaluate Immobilization Chemistry. *ACS Omega* **2018**, *3*, 8253−8259.
(44) Rao, C. N. R.; Kulkarni, G. U.; Thomas, P. J.; Edwards, P. P. Metal Nanoparticles and Their Assemblies. *Chem. Soc. Rev.* **2000**, *29*, 27−35.
(45) Khlebtsov, N. G.; Bogatyrev, V. A.; Dykman, L. A.; Melnikov, A. G. Spectral Extinction of Colloidal Gold and Its Biospecific Conjugates. *J. Colloid Interface Sci.* **1996**, *180*, 436−445.
(46) Pollitt, M. J.; Buckton, G.; Piper, R.; Brocchini, S. Measuring Antibody Coatings on Gold Nanoparticles by Optical Spectroscopy. *RSC Adv.* **2015**, *5*, 24521−24527.
(47) Dolinsky, T. J.; Nielsen, J. E.; McCammon, J. A.; Baker, N. A. Pdb2pqr: An Automated Pipeline for the Setup of Poisson-Boltzmann Electrostatics Calculations. *Nucleic Acids Res.* **2004**, *32*, W665−W667.
(48) Filipe, V.; Hawe, A.; Jiskoot, W. Critical Evaluation of Nanoparticle Tracking Analysis (Nta) by Nanosight for the Measurement of Nanoparticles and Protein Aggregates. *Pharm. Res.* **2010**, *27*, 796−810.

https://dx.doi.org/10.1021/acs.langmuir.1c00100
Langmuir XXXX, XXX, XXX−XXX